Planta (2020) 251:104
https://doi.org/10.1007/s00425-020-03396-0

ORIGINAL ARTICLE

Artificially lignified cell wall catalyzed by peroxidase selectively localized on a network of microfibrils from cultured cells

Seiya Hirano[1] · Yusuke Yamagishi[2] · Satoshi Nakaba[1] · Shinya Kajita[3] · Ryo Funada[1] · Yoshiki Horikawa[1]

Received: 5 September 2019 / Accepted: 29 April 2020 / Published online: 7 May 2020

Abstract

Main conclusion **An artificial lignified cell wall was synthesized in three steps: (1) isolation of microfibrillar network; (2) localization of peroxidase through immunoreaction; and (3) polymerization of DHP to lignify the cell wall.**

Abstract Artificial woody cell wall synthesis was performed following the three steps along with the actual formation in nature using cellulose microfibrils extracted from callus derived from *Cryptomeria japonica*. First, we constructed a polysaccharide network on a transmission electron microscopy (TEM) grid. The preparation method was optimized by chemical treatment, followed by mechanical fibrillation to create a microfibrillated network. Morphology was examined by TEM, and chemical characterization was by Fourier transform infrared (FTIR) spectroscopy. Second, we optimized the process to place peroxidase on the microfibrils via an immunoreaction technique. Using a xyloglucan antibody, we could ensure that gold particles attached to the secondary antibodies were widely and uniformly localized along with the microfibril network. Third, we applied the peroxidase attached to secondary antibodies and started to polymerize the lignin on the grid by simultaneously adding coniferyl alcohol and hydrogen peroxide. After 30 min of artificial lignification, TEM observation showed that lignin-like substances were deposited on the polysaccharide network. In addition, FTIR spectra revealed that the bands specific for lignin had increased, demonstrating the successful artificial formation of woody cell walls. This approach may be useful for studying woody cell wall formation and for producing made-to-order biomaterials.

Keywords Cellulose · FTIR · Hemicellulose · Immunoreaction · TEM

Abbreviations

DHP Dehydrogenation polymer
FTIR Fourier transform infrared
HRP Horseradish peroxidase
TEM Transmission electron microscopy

Communicated by Dorothea Bartels.

Electronic supplementary material The online version of this article (https://doi.org/10.1007/s00425-020-03396-0) contains supplementary material, which is available to authorized users.

✉ Yoshiki Horikawa
horikaw@cc.tuat.ac.jp

[1] Institute of Agriculture, Tokyo University of Agriculture and Technology, Fuchu, Tokyo 183-8509, Japan

[2] Research Faculty of Agriculture, Hokkaido University, Sapporo, Hokkaido 060-8589, Japan

[3] Graduate School of Bio-Applications and Systems Engineering, Tokyo University of Agriculture and Technology, Koganei, Tokyo 184-8588, Japan

Introduction

Lignified cell wall is the main substance of woody biomass that provides mechanical support for large trees, enabling them to live up to more than 1000 years. Lignified cell walls are divided into primary and secondary cell walls that differ in their chemical composition and microstructure. The peripheral cambium generates cells during cell division, after which the primary cell wall is formed. The cells are then expanded longitudinally and radially, and the final size is determined by the orientation of cellulose microfibrils that are produced by the cellulose synthase complex localized in the plasma membrane (Kimura et al. 1999). The secondary cell wall begins to form by the alignment of cellulose microfibrils; it consists of three layers, called S_1, S_2, and S_3, each of which is differentiated by the angle of its microfibrils (Kataoka et al. 1992; Abe et al. 1991).

Hemicelluloses accumulate in the cell wall, thereby providing mechanical strength by interacting with cellulose microfibrils through hydrogen bonding (Busse-Wicher

et al. 2014). In the secondary cell wall of softwoods, galactoglucomannan, followed by arabino-4-*O*-methylglucuronoxylans, are the most abundant components, whereas *O*-acetyl-4-*O*-methylglucuronoxylans are the main components in hardwoods (Fengel and Wegener 1989). The main hemicellulosic polysaccharide found in the primary cell wall is xyloglucan, in both softwoods and hardwoods. Xyloglucan links non-covalently to cellulose, causing the association of adjacent cellulose microfibrils, the main tension-bearing structures in the primary wall (McCann et al. 1990; Nishitani and Tominaga 1992). Pectin is regarded to have an important role in regulating cell wall extensibility by the formation of intermolecular bonds through the involvement of calcium ions (Higuchi et al. 1971; Guglielmino et al. 1997). In vitro experiments have demonstrated that these polysaccharides influence the crystalline structure of cellulose, its accumulation, and morphology (Tokoh et al. 1998, 2002).

Lignin deposition occurs in the compound middle lamella when the S_1 layer is formed (Takabe et al. 1981; Kiyoto et al. 2015). As secondary cell wall formation progresses, lignification proceeds from the outer layers and the entire cell wall becomes lignified. Biosynthesis of lignin occurs via the radical coupling of monolignols and is catalyzed by peroxidase or laccase (Zhao et al. 2013), after which non-condensed units, mostly containing 8-*O*-4′ aryl-ether bonds, are constructed (Terashima et al. 2009). Regarding the spatial deposition of lignin, it is to be expected that the peroxidase localizes close to hemicelluloses in the living cell wall. Support for this hypothesis comes from a study in which a *Zinnia* cell culture differentiated into tracheid elements at the points where peroxidase was localized in the secondary cell wall (Sato et al. 2006).

To study lignin biosynthesis and its chemical structure, dehydrogenation polymers (DHP), which are artificially synthesized from monolignols by the endwise polymerization method "Zutropfverfahren," have been investigated. However, such in vitro polymers possess much higher levels of condensed linkages that render them clearly different from lignins in living cells (Jacquet et al. 1997). Researchers have demonstrated that the chemical structure of lignin is altered by the accumulation of hemicelluloses. The 8-*O*-4′ linkage in DHP was increased under the influence of polysaccharides, such as hemicellulose (Higuchi et al. 1971) or pectin (Terashima et al. 1995, 1996) under aqueous conditions. Although several reports based on experiments using non-crystalline polysaccharides and lignin have been described, the process of cell wall formation remains unclear. Therefore, in vitro experiments have been explored using model cellulose. Li et al. (2015) established lignified cell wall synthesis based on bacterial cellulose; they used this method to investigate the structural modification of lignin by hemicelluloses. However, they did not use the cellulose microfibrils extracted from terrestrial plants. Furthermore, they added peroxidase to the reaction liquor to freely catalyze monolignol polymerization. This approach differs from ours, which is based on the hypothesis that the enzymes in living cells are localized close to polysaccharides.

Given this background, we investigated woody cell wall synthesis in vitro based on microfibrils from terrestrial plant cellulose. We focused on the hypothesis that peroxidase localizes close to hemicelluloses; therefore, the process of cell wall synthesis was divided into three steps based on what is known about its in vivo formation. Our process uses cellulose microfibrils extracted from callus derived from *Cryptomeria japonica* (Fig. 1). First, we constructed a polysaccharide network on a TEM grid. Second, the process was optimized to localize peroxidase close to the microfibrils through immunoreaction using antibody binding with gold particles. Third, artificial lignification was achieved by feeding monolignols and hydrogen peroxide (H_2O_2), which is catalyzed by peroxidase. The products obtained at each step were chemically and morphologically characterized by Fourier transform infrared (FTIR) spectroscopy and/or TEM observation.

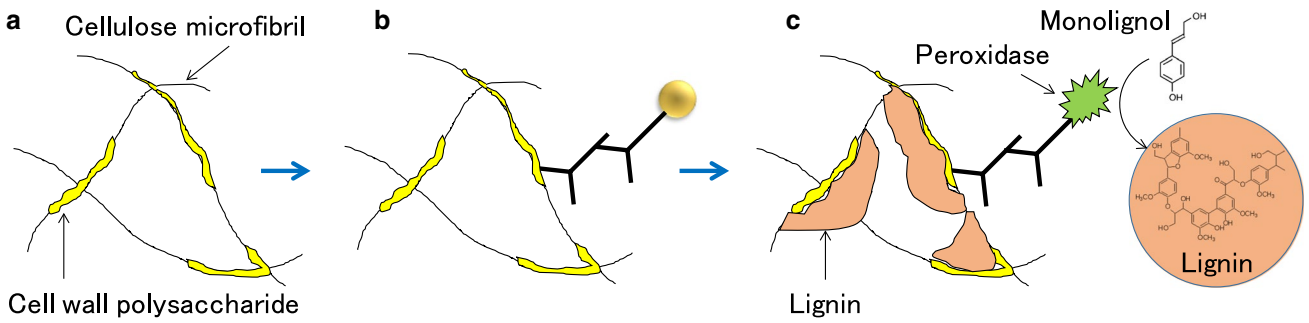

Fig. 1 Process of lignified cell wall synthesis. **a** Isolation of microfibrillar network with cell wall polysaccharides on the surface. **b** Optimization of the process to localize peroxidase close to the microfibrils via an immunoreaction using an antibody conjugated with a gold particle. **c** Artificial lignification catalyzed by on-site peroxidase, attached via an analogous antibody (without the gold particle)

Materials and methods

Induction of cell culture

Callus tissue was obtained from *Cryptomeria japonica* according to a published method (Yamagishi et al. 2015). The young needles from a *C. japonica* tree growing on the campus of the Tokyo University of Agriculture and Technology (Fuchu, Tokyo) were used for the induction of calli. These were placed on an improved Murashige and Skoog's medium (Murashige and Skoog 1962); 30 g of sucrose, 0.4 mg of thiamin hydrochloride, 2.5 mL of 2 mmol/l 2,4-dichlorophenoxyacetic acid, and 0.5 mL of 2 mmol/L benzyl amino purine were added. We applied 0.2% gellan gum to solidify the medium after adjusting the pH to 5.8 (Nakagawa et al. 2006). The induced callus was transferred to a new batch of the same medium, and incubated at 25 °C in darkness; subcultures were prepared in the same medium at 4–6-week intervals.

Polarized microscopic observation

The callus was put on the slide glass and observed by bright-field or polarized-light microscopy (Axioskop, Carl Zeiss, Oberkochen, Germany).

Cellulose purification

The callus-derived cellulose was purified according to our prior method (Horikawa 2017). The callus was directly immersed overnight in 5% KOH, without powdering it, at room temperature. After washing in distilled water, samples were subjected to sodium chlorite oxidation in water at pH 4–5 and 70 °C for 1 h to remove any lignin; this treatment is, hereafter, referred to as the 'Wise Treatment' (Wise et al. 1946). This delignification process was repeated three times. The products were then boiled in 5% KOH for 2 h to remove most of the hemicelluloses, some amorphous cellulose, and other non-cellulosic components. The cellulose purification process was monitored by IR spectroscopy, as described below. The products obtained were washed in distilled water and subsequently used for artificial cell wall synthesis.

For preparing cellulose sample from the woody powder of *C. japonica*, woody chips of *C. japonica* were milled by two-step grinding, using an Orient mill (VM-16, Seishin Enterprise Corp., Tokyo, Japan) followed by Bantam mill AP-BL (Hosokawa Micron, Osaka, Japan); the products were treated using the Wise method to remove lignin. The treatment was repeated and the samples were treated with 5% NaOH for 2 h. The products obtained were washed in distilled water.

IR spectroscopy

FTIR spectra were obtained using a PerkinElmer Frontier system (Waltham, MA, USA) equipped with the Spotlight 200i FTIR Microscope System, in the 4000–750 cm^{-1} range. The spectra were recorded with a spectral resolution of 4 cm^{-1} and acquisition of 128 scans, using a low-noise HgCdTe detector that was cooled to − 196 °C with liquid nitrogen. To monitor cellulose purification, the sample suspension was placed on a BaF_2 window (13 mm diameter × 2 mm thickness) and dried completely for spectral measurement. To detect lignin synthesis, the TEM grid was set directly onto the sample holder for spectral acquisition.

X-ray diffraction analysis

Freeze-dried cellulose samples were molded into pellets using a hand press machine for X-ray diffraction analysis. X-ray diffractograms were obtained in the reflection mode using Cu–Kα radiation ($\lambda = 1.5418$ Å) from an UltraX-18HF diffractometer (Rigaku Corp., Tokyo, Japan) at 40 kV and 300 mA. The full width at half maximum was evaluated from the diffraction peak (2 0 0) around 22.4° to understand the crystalline feature of the cellulose sample.

Transmission electron microscopy (TEM)

Microfibrillated cellulose was prepared from callus cellulose using a Hiscotron double-cylinder-type homogenizer (Microtec, Chiba, Japan). Droplets of the cellulose suspension were placed on a copper grid or nickel grid for immunoreaction (Okenshoji, Tokyo, Japan), which had been covered by a carbon film. After negative staining with 2% uranyl acetate, TEM observation was carried out using a JEM-1400 Plus TEM (JEOL, Tokyo, Japan) at 80 kV. The microfibril width was estimated from the image using the commercial software, ImageJ.

Immunoreaction using a primary antibody for a non-cellulosic polysaccharide

Microfibrillated cellulose was spotted onto the grid that was supported by a carbon film. After treating the grid in 1 M saline sodium citrate buffer (pH 7.0, containing 1% bovine serum albumin) at room temperature for 30 min as a blocking treatment, the grids were incubated in anti-xylan (LM11) (McCartney et al. 2005), anti-homogalacturonan (LM18) (Verhertbruggen et al. 2009), or anti-xyloglucan (LM25) (Pedersen et al. 2012) antibodies (PlantProbes, Leeds, UK) (at 1:500 dilution in the corresponding buffer) for 2 h at room temperature or overnight at 4 °C. After three washings with the buffer for 15 min, the grids were reacted with goat anti-rat secondary antibody conjugated with 5 nm colloidal

gold particles (BBI Solutions, Sittingbourne, UK) for 2 h at room temperature (at 1:20 dilution in corresponding buffer). For the control, microfibrillated cellulose was reacted with only the secondary antibody. Finally, the grids were washed in three changes of the buffer for 15 min and then washed in distilled water. For artificial lignin synthesis, we applied the secondary antibody bound with horseradish peroxidase (HRP) (Jackson ImmunoResearch Inc., West Grove, PA, USA) instead of gold particles. In 30 mL of the corresponding buffer, we then dissolved 12 mg of freeze-dried powder of the antibody bound to HRP; this was defined as the reaction liquid, and it included the secondary antibody.

Dehydrogenation polymer (DHP) synthesis

DHP was synthesized according to a published method (Grabber et al. 2003): 12 mM coniferyl alcohol and 2 mM H_2O_2 were simultaneously delivered by adding droplets to HRP, which then became attached to the microfibrillated cellulose on the TEM grid at room temperature. The products were washed with distilled water several times before negative staining for the TEM observation.

Results

We examined woody cell wall synthesis using plant cellulose microfibrils. We concluded that we have successfully designed artificial lignified cell walls, in three steps: (1) isolation of a microfibrillated cellulose network, (2) optimization of the process for localizing peroxidase using immunoreaction, and (3) polymerization of DHP to lignify the cell wall on the TEM grid.

Isolation of polysaccharide network

To prepare the polysaccharide network for the isolation of artificial lignified plant cell wall (Fig. 1a), callus derived from *C. japonica* was employed. The cultured cells viewed under polarized light showed clear birefringence, which indicated that crystalline cellulose microfibrils had accumulated in the cell walls (Fig. S1). Terrestrial plant cellulose microfibrils are easily shortened by acid hydrolysis (Horikawa et al. 2018); therefore, to extract cellulose from the callus while retaining the longer fibers, the samples were treated without acidic chemicals. The FTIR microscopic spectra, in the range of 1800–800 cm^{-1}, of the callus during the cellulose purification process are presented in Fig. 2. Before chemical treatment, the band at 1508 cm^{-1} (Horikawa et al. 2019), ascribed to aromatic skeletal vibrations, was not visible, indicating that little lignin was deposited in the callus cell wall (Fig. 2a); after treatment with 5% KOH overnight, the bands at 1650 and 1550 cm^{-1}, assigned to C=O-stretching and N–H-bending vibrations due to protein, were reduced (Fig. 2b). Repeated Wise treatment accelerated the removal of protein, whereas the bands around 1600 cm^{-1}, ascribed to carboxylate, remained (Fig. 2c). After treatment in boiling 5% KOH, a typical spectral pattern of cellulose was obtained (Horikawa 2017), although there was little absorbance around 1600 cm^{-1} (Fig. 2d). The X-ray diffractograms of purified cellulose prepared from the callus and woody powder of *C. japonica* are shown in Fig. S2. The full width at half maximum of at the peak (200) can be used to assess cellulose crystallinity, and the values become higher with lower crystalline cellulose microfibril based on Scherrer's equation. The value from callus cellulose was 3.46, which is notably higher than that of the woody powder, at 2.55 (Horikawa 2017), indicating that cellulose crystallinity prepared from woody powder was better than that from callus cellulose. The higher cellulose crystallinity of the woody powder is due to the fact that it consists mainly of secondary cell wall, including highly aligned microfibrils, whereas callus cellulose consists of primary cell wall.

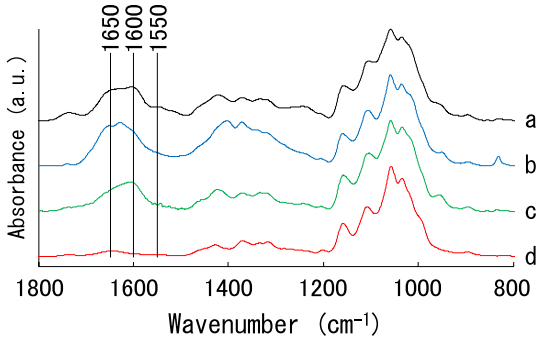

Fig. 2 FTIR spectra of *Cryptomeria japonica* callus samples in the range of 1800–800 cm^{-1}. **a** Before and **b** after 5% KOH treatment at room temperature, followed by **c** Wise treatment three times and then **d** boiling in 5% KOH. The bands at 1650 and 1550 cm^{-1} are assigned to C=O-stretching and N–H-bending vibrations from proteins. The band at 1600 cm^{-1} is ascribed to stretching vibrations due to carboxylates

Mechanical treatment employing a double-cylinder-type homogenizer was used to prepare microfibrillated cellulose from purified callus cellulose (Fig. 3). The width of cellulose fibers was approximately 4 nm, which is consistent with that of terrestrial plant cellulose microfibrils (Saito et al. 2007). Therefore, the polysaccharide network constructed on the TEM grid under the above-mentioned chemical and mechanical processing was applied for the following experiment.

Optimization of the process for localizing peroxidase near the microfibril via immunoreaction

To match the process of in vivo cell wall formation, an immunoreaction was used to place the enzyme adjacent

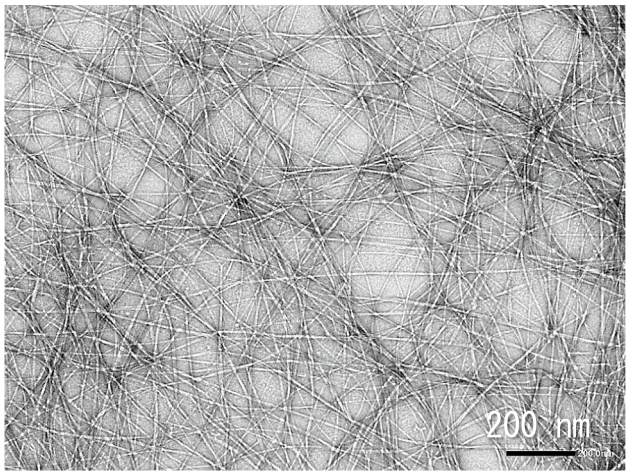

Fig. 3 Transmission electron microscopy image of *Cryptomeria japonica* callus cellulose microfibrils after mechanical treatment

to the polysaccharide network (Fig. 1b). To determine the appropriate primary antibody, we examined reactions using several anti-hemicellulose or anti-pectin antibodies. A secondary antibody conjugated with 5 nm gold particles was used to evaluate the distribution under TEM observation. The negative control, in which only the secondary antibody was applied to the microfibrillar network, is shown in Fig. 4a. There were no gold particles detected adjacent to the microfibrils or on the surface of the grid. When the anti-xylan (LM11) antibody was applied, only a few gold particles were observed (Fig. 4b). This negative finding is consistent with what would be expected in a woody cell wall structure, because xylan accumulates mainly in the secondary cell wall (Kim et al. 2010a). Using an anti-pectin antibody (LM18), some gold particles were located near the cellulose microfibrils (Fig. 4c). The TEM observation was supported by the FTIR spectra, in which bands at around 1600 cm^{-1} became visible, indicating that pectin remained in the fraction after successive chemical treatments (Fig. 2d). When anti-xyloglucan antibodies were applied, more gold particles were uniformly observed on the cellulose microfibrillar network (Fig. 4d), consistent with xyloglucans being the main hemicellulose in the primary cell wall. To find the optimal antibody for this study, we used TEM images to assess the distance between gold particles and the microfibril surface (Fig. 4e). Using an anti-xyloglucan antibody, many gold particles were close to the microfibrils, at a distance of 14.2 ± 15.2 nm, with a narrow distribution of distances (Fig. 4f). Kimura et al. (1999) reported that the distance between gold particle and the antigen, using a primary and secondary antibody, is around 27.2 nm. Therefore, the average distance of 14.2 nm, within a narrow distance distribution, is consistent with specific recognition by the xyloglucan antibody. These results suggest that xyloglucan was localized on the surface of the cellulose microfibrillar network, even after successive chemical and mechanical treatments. We, therefore, concluded that the anti-xyloglucan antibody was the best tool to place peroxidase close to the microfibrillar network for artificial cell wall synthesis.

Artificial lignification catalyzed by on-site peroxidases

To complete the preparation of the artificially lignified cell wall (Fig. 1c), DHP was synthesized in the microfibrillated cellulose network on the TEM grid. After a blocking treatment, anti-xyloglucan was applied to the grid on which the microfibrillated cellulose network was constructed. Secondary antibody conjugated with peroxidase, instead of gold particle, was applied to the primary antibody on the TEM grid (Fig. 5a). A characteristic contrast was observed around the microfibrillar network, which was similar pattern in the binding of xyloglucan to gold particles through primary and secondary antibodies previously (Fig. 4d, e). To synthesize artificial lignin, solutions of coniferyl alcohol and H_2O_2 were simultaneously applied to the grid upon which the peroxidase was localized around the microfibrillar network via primary and secondary antibodies. After incubation for 30 min, new substances were observed, after which the microfibrillar morphology became electron-dense (Fig. 5b). When the sample was incubated for a longer time to synthesize artificial lignin, the microfibrillar morphology became entirely electron-dense, because these substances had entirely covered the microfibrillar network.

FTIR spectra were used to chemically assess the samples before and after artificial lignification. The grid for TEM observation without negative staining was placed in a microscope equipped with FTIR spectroscopy capability, and the sample was irradiated with infrared light. The FTIR spectra in which the bands at 1650 and 1550 cm^{-1}, ascribed to C=O-stretching and N–H-bending vibrations from proteins, can be seen and are presented in Fig. 6a. The presence of these particular bands can be explained by the fact that the primary and secondary antibodies conjugated with peroxidase were localized to the cellulose microfibrils (Fig. 5a). After incubation for 30 min, a new IR absorption was slightly visible around 1508 cm^{-1}, the band assigned to the aromatic skeletal vibration in lignin (Fig. 6b). When the DHP was synthesized for 12 h, the bands at 1508 and 1267 cm^{-1} (Fig. 6c), both of which are related to lignin (Faix 1991; Horikawa et al. 2019), increased. As a negative control experiment, lignin polymerization was examined by coniferyl alcohol without H_2O_2. The bands at 1508 and 1267 cm^{-1} ascribed to lignin were not seen in Fig. 6d, which was clearly different from Fig. 6c. Therefore, we were able to conclude that localized artificial lignification was catalyzed by peroxidases that were localized close to the microfibrillar network.

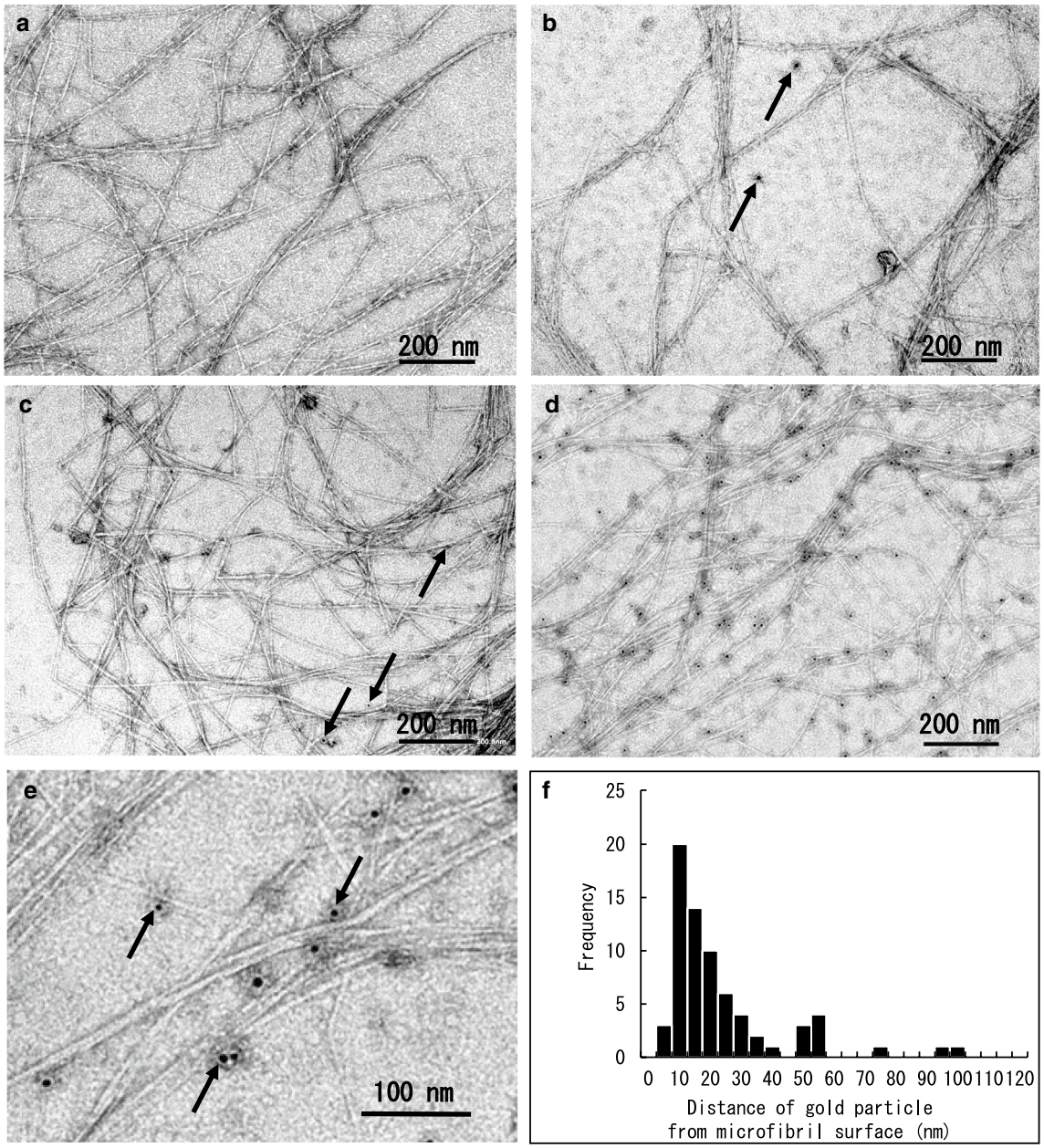

Fig. 4 TEM images of microfibrillar cellulose using antibodies that recognize various non-cellulosic polysaccharides. **a** Control in which only secondary antibody was used. **b** Anti-xylan. **c** Anti-pectin. **d** Anti-xyloglucan antibodies. **e** Enlarged image of (**d**). **f** Quantification of labeling distance of antibodies from the center of a gold particle to the microfibril. Arrows in **b**, **c**, and **e** indicate the gold particles bound with secondary antibodies

Discussion

In this study, we successfully developed an artificial lignified cell wall based on three steps. In the first step, a microfibrillated network was constructed on the TEM grid by a combination of chemical treatment with mechanical processing from the cultured cell wall. The width of cellulose fibers was approximately 4 nm (Fig. 3), which is consistent with that of cellulose microfibrils in the higher plants. However, when the cellulose suspension was prepared by mechanical processing from woody powder, the cellulose fibers obtained were 15–20 nm in width (Abe et al. 2007); this is because cellulose accumulated in the actual cell wall in the form of microfibril bundles. Plant callus cell walls consist mainly of the primary wall, in which cellulose microfibrils, rather than microfibril bundles, are accumulated. Hult et al. (2003) have successfully prepared dispersed microfibrils from holocellulose; the hemicellulose appeared to prevent aggregation

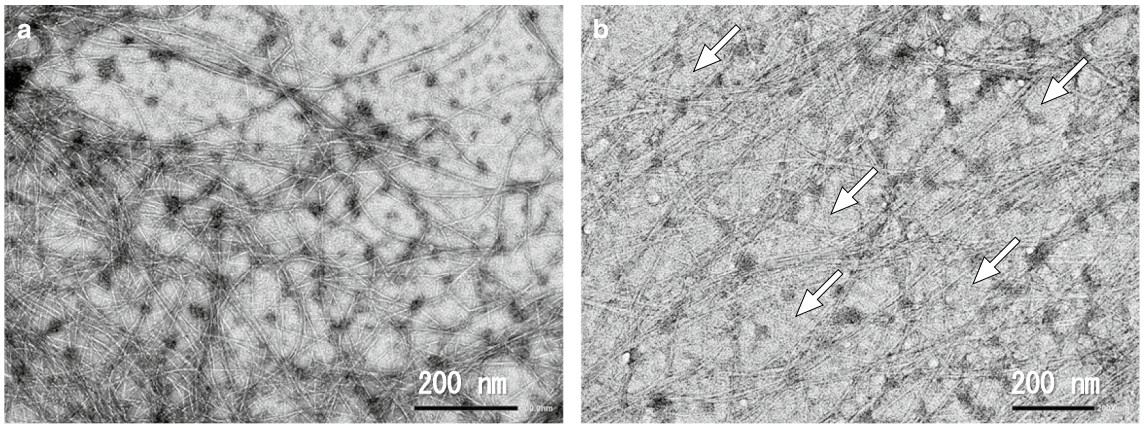

Fig. 5 Dehydrogenation polymer (DHP) synthesis using peroxidases that were localized to the microfibrils via xyloglucan and peroxidase-attached anti-xyloglucan antibodies. TEM observation images from **a** before and **b** after DHP synthesis for 30 min. Arrows in **b** indicate new substances among the microfibrils

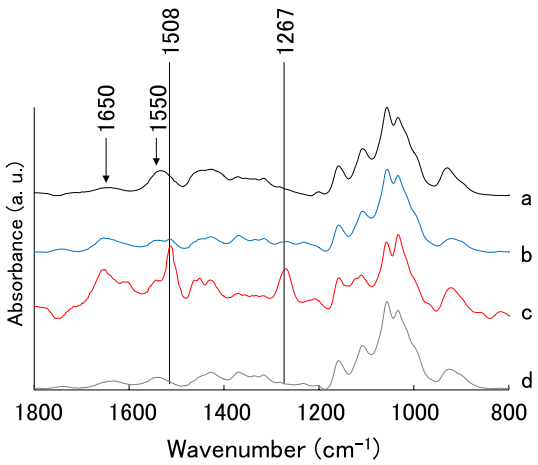

Fig. 6 Dehydrogenation polymer synthesis using peroxidases that were localized to the microfibrils through xyloglucan (as in Fig. 5). FTIR spectra in the range 1800–800 cm^{-1}: **a** before, **b** 30 min, and **c** 12 h after DHP synthesis. **d** Negative control for dehydrogenation polymer synthesis after adding coniferyl alcohol alone. The bands at 1650 and 1550 cm^{-1} are assigned to C=O-stretching and N–H-bending vibrations from proteins. The bands at 1508 and 1267 cm^{-1} are ascribed to aromatic skeletal vibrations and C–O stretching due to lignin, respectively

of microfibrils. Saito et al. (2007) successfully developed a highly dispersed microfibril suspension using the chemical radical TEMPO (2,2,6,6-tetramethylpiperidine 1-oxyl). Selective C-6 oxidation occurred on the microfibrillar surface; the resulting anionic carboxylate groups caused electrostatic repulsion between the TEMPO-oxidized cellulose microfibrils, resulting in a significant dispersion (Saito et al. 2007).

In our study, we found that hemicelluloses and/or carboxylates within pectin may help to effectively disperse microfibrils; this may be supported by the small absorption which we observed at around 1600 cm^{-1} (Fig. 2d); the band ascribed to carboxylic acids (Horikawa et al. 2019). We also examined the sample after 5% KOH + Wise treatment but without boiling in 5% KOH for 2 h, corresponding to the spectra in Fig. 2c. After mechanical treatment, the cellulose microfibrils were significantly dispersed under TEM observation (Fig. S3). However, an unknown substrate, possibly a non-cellulosic polysaccharide, between the microfibrils was also observed. Following artificial lignification on this microfibrillar network, the synthesized lignin could not be differentiated from the non-cellulosic polysaccharide under TEM; therefore, we concluded that the microfibril samples, as shown in Figs. 2d and 3, provided the required scaffold for artificial cell wall production.

In the second step, we determined the optimum condition of immunoreaction to localize enzymes close to microfibrils, resulting in successful lignification. In this study, the best primary antibody was anti-xyloglucan that is the main hemicellulose accumulated in the cultured cell (Fig. 4d, e). Kim et al. have reported the temporal and spatial immunolocalization of glucomannan and xylan using these specific antibodies. Therefore, when the polysaccharide network was prepared on the TEM grid from softwood, anti-glucomannan or anti-xylan should be applied for an artificial lignified cell wall catalyzed by peroxidase. Furthermore, the amount of lignin deposited in the polysaccharide network can be controlled by changing the concentration of these primary antibodies, which is the potential of our artificial cell wall synthesis system.

In the third step, by applying monolignol and H_2O_2, an achievement of lignification using peroxidases that were localized to the microfibrils through immunoreaction was clearly confirmed by TEM observation and FTIR spectral analysis (Figs. 5 and 6). For the artificial lignification, the addition of only coniferyl alcohol or only H_2O_2 (the negative

control) did not alter the microfibrillar network morphology (Fig. S4a, b). FTIR spectra after lignin polymerization were clearly different from those produced by coniferyl alcohol alone (Fig. 6d), demonstrating that the unreacted monomer did not remain on the grid. Given the above-mentioned control experiment, we can confirm the synthesis of the artificial lignified cell wall catalyzed by peroxidase selectively localized on a network of microfibrils by immunoreaction.

Conclusions

The structure of lignin is influenced by the presence of polysaccharides, such as hemicelluloses and pectin. We successfully designed an artificially lignified cell wall, using three steps: first, isolation of a microfibrillar network; second, localization of peroxidase through immunoreaction; and third, polymerization of DHP to lignify the cell wall on a TEM grid. The approach has the potential to provide a better model for understanding cell wall formation, and for understanding the minimum requirements to produce a lignified cell wall. Furthermore, using dehydrogenation polymerization to produce our artificial cell wall may help to explain why non-condensed linkages in lignin are prevalent in living cells; in a future publication, we will report on the chemical attributes of the lignin produced using this approach. The ability to control cell wall formation may also help in the production of made-to-order biomaterial.

Author contribution statement SH and YH designed the research. SH, YY, SN and YH performed the experiments. SH, SK, RF and YH analyzed the data. SH and YH wrote the manuscript. All authors read and approved the manuscript.

Acknowledgements This research study was supported by the Japan Society for the Promotion of Science (JSPS) [KAKENHI Grant Nos. 17H03840 and 19K06167]. The authors express their sincere thanks to Prof. John Ralph from the University of Wisconsin for technical advice on synthesizing DHP and for helpful discussion.

Compliance with ethical standards

Conflict of interest The authors declare no conflict of interest.

References

Abe H, Ohtani J, Fukazawa K (1991) FE-SEM observations on the microfibrillar orientation in the secondary wall of tracheids. Iawa Bull 12:431–438. https://doi.org/10.1163/22941932-90000546

Abe K, Iwamoto S, Yano H (2007) Obtaining cellulose nanofibers with a uniform width of 15 nm from wood. Biomacromol 8:3276–3278. https://doi.org/10.1021/bm700624p

Busse-Wicher M, Gomes TCF, Tryfona T, Nikolovski N, Stott K, Grantham NJ, Bolam DN, Skaf MS, Dupree P (2014) The pattern of xylan acetylation suggests xylan may interact with cellulose microfibrils as a twofold helical screw in the secondary plant cell wall of *Arabidopsis thaliana*. Plant J 79:492–506. https://doi.org/10.1111/tpj.12575

Faix O (1991) Classification of lignins from different botanical origins by FT-IR spectroscopy. Holzforschung 45:21–27. https://doi.org/10.1515/hfsg.1991.45.s1.21

Fengel D, Wegener G (1989) Wood: chemistry, ultrastructure, reactions. Walter de Gruyter, Berlin

Grabber JH, Hatfield RD, Ralph J (2003) Apoplastic pH and monolignol addition rate effects on lignin formation and cell wall degradability in maize. J Agr Food Chem 51:4984–4989. https://doi.org/10.1021/jf030027c

Guglielmino N, Liberman M, Catesson AM, Mareck A, Prat R, Mutaftschiev S, Goldberg R (1997) Pectin methylesterases from poplar cambium and inner bark: localization, properties and seasonal changes. Planta 202:70–75. https://doi.org/10.1007/s004250050104

Higuchi T, Ogino K, Tanahashi M (1971) Effect of polysaccharides on dehydropolymerization of coniferyl alcohol. Wood Res 51:1–11

Horikawa Y (2017) Assessment of cellulose structural variety from different origins using near infrared spectroscopy. Cellulose 24:5313–5325. https://doi.org/10.1007/s10570-017-1518-0

Horikawa Y, Shimizu M, Saito T, Isogai A, Imai T, Sugiyama J (2018) Influence of drying of chara cellulose on length/length distribution of microfibrils after acid hydrolysis. Int J Biol Macromol 109:569–575. https://doi.org/10.1016/j.ijbiomac.2017.12.051

Horikawa Y, Hirano H, Mihashi A, Kobayashi Y, Zhai S, Sugiyama J (2019) Prediction of lignin contents from infrared spectroscopy: chemical digestion and lignin/biomass ratios of *Cryptomeria japonica*. Appl Biochem Biotechnol 188:1066–1077. https://doi.org/10.1007/s12010-019-02965-8

Hult EL, Iversen T, Sugiyama J (2003) Characterization of the supermolecular structure of cellulose in wood pulp fibres. Cellulose 10:103–110. https://doi.org/10.1023/A:1024080700873

Jacquet G, Pollet B, Lapierre C, Francesch C, Rolando C, Faix O (1997) Thioacidolysis of enzymatic dehydrogenation polymers from *p*-hydroxyphenyl, guaiacyl, and syringyl precursors. Holzforschung 51:349–354. https://doi.org/10.1515/hfsg.1997.51.4.349

Kataoka Y, Saiki H, Fujita M (1992) Arrangement and superimposition of cellulose microfibrils in the secondary walls of coniferous tracheids. Mokuzai Gakkaishi 38:327–335

Kim JS, Awano T, Yoshinaga A, Takabe K (2010a) Immunolocalization and structural variations of xylan in differentiating earlywood tracheid cell walls of *Cryptomeria japonica*. Planta 232:817–824. https://doi.org/10.1007/s00425-010-1225-7

Kim JS, Awano T, Yoshinaga A, Takabe K (2010b) Temporal and spatial immunolocalization of glucomannans in differentiating earlywood tracheid cell walls of *Cryptomeria japonica*. Planta 232:545–554. https://doi.org/10.1007/s00425-010-1189-7

Kimura S, Laosinchai W, Itoh T, Cui XJ, Linder CR, Brown RM (1999) Immunogold labeling of rosette terminal cellulose-synthesizing complexes in the vascular plant *Vigna angularis*. Plant Cell 11:2075–2085. https://doi.org/10.1105/tpc.11.11.2075

Kiyoto S, Yoshinaga A, Takabe K (2015) Relative deposition of xylan and 8–5′-linked lignin structure in *Chamaecyparis obtusa*, as revealed by double immunolabeling by using monoclonal antibodies. Planta 241:243–256. https://doi.org/10.1007/s00425-014-2181-4

Li Q, Koda K, Yoshinaga A, Takabe K, Shimomura M, Hirai Y, Tamai Y, Uraki Y (2015) Dehydrogenative polymerization of coniferyl alcohol in artificial polysaccharides matrices: Effects of xylan on

the polymerization. J Agr Food Chem 63:4613–4620. https://doi.org/10.1021/acs.jafc.5b01070
McCann MC, Wells B, Roberts K (1990) Direct visualization of cross-links in the primary plant-cell wall. J Cell Sci 96:323–334
McCartney L, Marcus SE, Knox JP (2005) Monoclonal antibodies to plant cell wall xylans and arabinoxylans. J Histochem Cytochem 53:543–546. https://doi.org/10.1369/jhc.4B6578.2005
Murashige T, Skoog FK (1962) A revised medium for rapid growth and bio-assays with tobacco tissue cultures. Physiol Plant 15:473–497. https://doi.org/10.1111/j.1399-3054.1962.tb08052.x
Nakagawa R, Ogita S, Kubo T, Funada R (2006) Effect of polyamines and L-ornithine on the development of proembryogenic masses of *Cryptomeria japonica*. Plant Cell Tiss Org 85:229–234. https://doi.org/10.1007/s11240-006-9076-4
Nishitani K, Tominaga R (1992) Endo-xyloglucan transferase, a novel class of glycosyltransferase that catalyzes transfer of a segment of xyloglucan molecule to another xyloglucan molecule. J Biol Chem 267:21058–21064
Pedersen HL, Fangel JU, McCleary B, Ruzanski C, Rydahl MG, Ralet MC, Farkas V, von Schantz L, Marcus SE, Andersen MCF, Field R, Ohlin M, Knox JP, Clausen MH, Willats WGT (2012) Versatile high resolution oligosaccharide microarrays for plant glycobiology and cell wall research. J Biol Chem 287:39429–39438. https://doi.org/10.1074/jbc.M112.396598
Saito T, Kimura S, Nishiyama Y, Isogai A (2007) Cellulose nanofibers prepared by TEMPO-mediated oxidation of native cellulose. Biomacromol 8:2485–2491. https://doi.org/10.1021/bm0703970
Sato Y, Demura T, Yamawaki K, Inoue Y, Sato S, Sugiyama M, Fukuda H (2006) Isolation and characterization of a novel peroxidase gene ZPO-C whose expression and function are closely associated with lignification during tracheary element differentiation. Plant Cell Physiol 47:493–503. https://doi.org/10.1093/pcp/pcj016
Takabe K, Fujita M, Harada H, Saiki H (1981) Lignification process of Japanese black pine (*Pinus thunbergii* Parl.) tracheids. Mokuzai Gakkaishi 12:813–820
Terashima N, Atalla RH, Ralph SA, Landucci LL, Lapierre C, Monties B (1995) New preparations of lignin polymer models under conditions that approximate cell-wall lignification. 1. Synthesis of novel lignin polymer models and their structural characterization by ^{13}C NMR. Holzforschung 49:521–527
Terashima N, Atalla RH, Vanderhart DL (1996) Solid state NMR of specifically ^{13}C-enriched lignin in wheat straw. Phytochemistry 46:863–870. https://doi.org/10.1016/S0031-9422(97)00359-2
Terashima N, Akiyama T, Ralph S, Evtuguin D, Pascoal Neto C, Parkås J, Paulsson M, Westermark U, Ralph J (2009) 2D-NMR (HSQC) difference spectra between specifically ^{13}C-enriched and unenriched protolignin of *Ginkgo biloba* obtained in the solution state of whole cell wall material. Holzforschung 63:379–384. https://doi.org/10.1515/HF.2009.074
Tokoh C, Takabe K, Fujita M, Saiki H (1998) Cellulose synthesized by *Acetobacter xylinum* in the presence of acetyl glucomannan. Cellulose 5:249–261. https://doi.org/10.1023/A:1009211927183
Tokoh C, Takabe K, Sugiyama J, Fujita M (2002) Cellulose synthesized by *Acetobacter xylinum* in the presence of plant cell wall polysaccharides. Cellulose 9:65–74. https://doi.org/10.1023/A:1015827121927
Verhertbruggen Y, Marcus SE, Haeger A, Ordaz-Ortiz JJ, Knox JP (2009) An extended set of monoclonal antibodies to pectic homogalacturonan. Carbohydr Res 344:1858–1862. https://doi.org/10.1016/j.carres.2008.11.010
Wise L, Murphy M, D'Addieco A (1946) Chlorite holocellulose, its fractionation and beating on summative wood analysis and studies on the hemicelluloses. Pap Trade J 122:35–43
Yamagishi Y, Uchiyama H, Sato T, Kitamura K, Yoshimoto J, Nakaba S, Watanabe U, Funada R (2015) In vitro induction of the formation of tracheary elements from suspension-cultured cells of the conifer *Cryptomeria japonica*. Trees-Struct Funct 29:1283–1289. https://doi.org/10.1007/s00468-014-1139-2
Zhao Q, Nakashima J, Chen F, Yin YB, Fu CX, Yun JF, Shao H, Wang XQ, Wang ZY, Dixon RA (2013) Laccase is necessary and nonredundant with peroxidase for lignin polymerization during vascular development in *Arabidopsis*. Plant Cell 25:3976–3987. https://doi.org/10.1105/tpc.113.117770